Progress towards a transportable laser-cooled Yb^+ microwave clock

Michael A. Trigatzis, Martin Knapp, Sean Mulholland, Gary I. Hockley, Geoffrey P. Barwood, Guilong Huang, Hugh A. Klein, Patrick Gill
Time and Frequency Department
National Physical Laboratory
Teddington, UK
michael.trigatzis@npl.co.uk

We present progress towards a transportable laser-cooled ytterbium ion microwave clock. We have designed and built a new trap chamber which we describe in this paper. Initial results of Rabi spectroscopy and clock stability are presented, and the next steps are outlined.

Keywords—microwave clock, ytterbium, ion trap, transportable atomic clock

I. INTRODUCTION

Optical atomic clocks based on cold atoms or ions represent the current state of the art in terms of clock stability and accuracy. However, they are difficult to commercialise since they rely on high size, weight, power and cost (SWAP-C) subsystems including optical frequency combs and ultranarrow-linewidth lasers. Laser-cooled ion microwave clocks offer performance advantages in long-term frequency stability and reproducibility, in comparison to current commercially available clocks, without needing high SWaP-C optical subsystems [1-3]. Their relative simplicity and high performance make them excellent candidates for applications including navigation and as master clocks in critical national timing infrastructures.

II. SYSTEM OVERVIEW

The prototype NPL Yb^+ microwave clock is composed of the electronics, lasers and optics, and physics package systems. These are described below.

The electronics have been described previously [1, 4], so we only give a brief overview here. The frequency chain starts with a 10 MHz oven-controlled crystal oscillator (OCXO) which serves as the clock's local oscillator referencing a direct digital synthesizer (DDS). This DDS generates the 12.6 GHz microwave signal used for the clock. After interrogating the ions, an error signal is generated in software and a correction is applied to the DDS output. An equivalent offset is added to a 12.8 GHz signal that is multiplied up from the free-running OCXO; this signal is then divided down to give the clock output. Between the DDS and microwave antenna we have a pair of single-pole, double-throw microwave switches and a series of attenuators. These allow us to quickly switch between 3 microwave states: high power for laser cooling, low power for spectroscopy, and minimum power. The minimum power state is used to optically pump ions into the hyperfine ground state ($F = 0$) and to detect ions in the $F = 1$ level of the electronic ground state. The residual microwave power in the minimum power state currently limits the length of the pi-pulses and prohibits Ramsey spectroscopy.

Three lasers are used to ionize, trap, cool, optically pump and detect ytterbium-171 ions. In our test setup, the two UV lasers at 369 nm and 399 nm are extended-cavity diode lasers (ECDLs). The former is used for laser cooling, optical pumping, and detection on the $^2S_{1/2} \rightarrow {}^2P_{1/2}$ transition. The latter is used when loading the ion trap by exciting the $^1S_0 \rightarrow {}^1P_1$ transition in neutral ytterbium. The UV lasers are combined using a dichroic mirror and coupled into a polarization-maintaining fibre. To repump ions which fall into the $^2D_{3/2}$ state, we use a 935 nm distributed Bragg reflector (DBR) laser. The IR beam is combined with the UV close to the physics package and aligned through the vacuum chamber. Fluorescence from the ions is detected using a lens system that includes a spatial filter and photomultiplier tube (PMT); a simplified schematic of the optics and physics package is shown in Fig. 1.

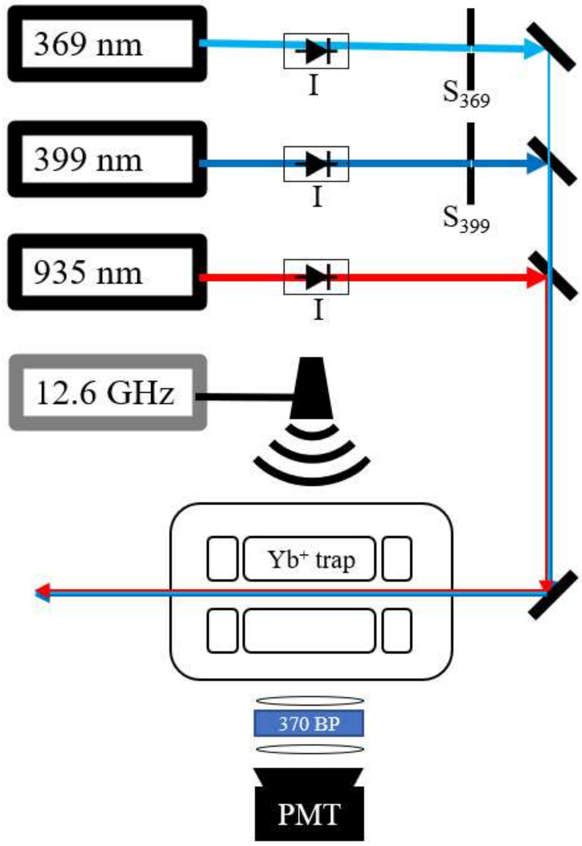

Fig. 1. Schematic of the experimental setup. The lasers are combined and pass through the ion trap that is also being radiated by microwaves at 12.6 GHz. The fluorescence from the ions is collected through a system of lenses and filters. The labels on the diagram are as follows: I – isolator, S_{369}, S_{399} – shutters for the 369 and 399 nm lasers, 370 BP – 370 ±10 nm bandpass filter, PMT – photomultiplier tube.

We acknowledge the support of the UK government department for Science, Innovation and Technology through the UK national quantum technologies program.

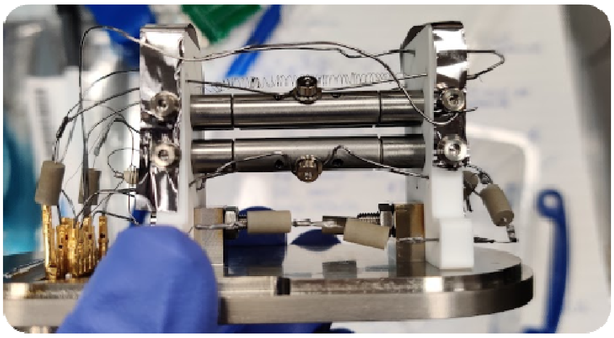

Fig. 2. The ion trap is formed of 4 segmented 6-mm diameter rods. The central rods have a length of 25 mm, and the ends are 10 mm. The ion-rod spacing is 2.6 mm.

III. Ion Trap and Physics Package Design

The trap and vacuum system are the key components in a laser-cooled trapped ion clock. To get the best clock performance, the ion trap should be designed to hold many ions and maintain a low ion-heating rate. In addition to these requirements for the trapping potential, there should also be sufficient optical access for the required laser beams and detecting the state of the ions. To enable long ion lifetime the vacuum level should be at or below 10^{-10} mbar.

The new ion trap and vacuum chamber are shown respectively in Fig. 2 and Fig. 3.

The trap (a linear quadrupole trap) is built on the lid of the chamber that contains the electrical feedthrough. The ion trap is formed of 4 segmented 6-mm diameter rods that are supported from either end by two ceramic spacers with a central bore that allows lasers to pass along the trap axis. The central rods have a length of 25 mm, and the end rods are 10 mm. The non-evaporable getters with integrated heaters are also supported by ceramic spacers and connected

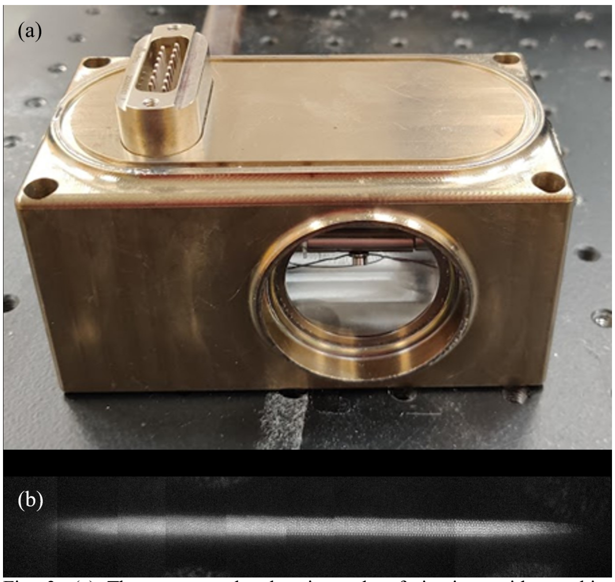

Fig. 3. (a) The vacuum chamber is made of titanium with sapphire viewports. The outer dimensions are 60 x 60 x 110 mm^3. (b) Composite image of a large Coulomb crystal of approx. 13,500 ions. Individual ions are visible in the in-focus section of the image to the lower side. The length of the ion crystal in the image is 3.5 mm.

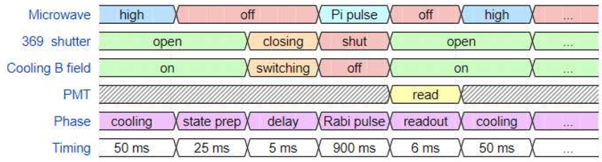

Fig. 4. Timing diagram showing the sequence used for Rabi spectroscopy.

to the electrical feedthrough.

This lid is welded into the titanium chamber body that contains welded-in sapphire viewports. The materials used for the trap structure and the viewports facilitate baking the vacuum chamber to a high temperature.

A cold crystal of ions, up to 10 mm in length, is trapped at the centre of the trap and is typically made up of tens of thousands of ions. An example of an ion crystal is shown on Fig. 3(b). To load the ions, an oven containing ytterbium is heated and the 399-nm laser photoionizes the atoms [2]. After this step, the shutter for the 399-nm laser is closed. Ion storage times are in the range of days to weeks which is a significant improvement over the few-hours of our previous system [1].

The trap chamber is placed inside a two-layer mu-metal magnetic shield which reduces the ambient field by a factor of over 250 in all three directions. Microwaves are delivered to the ions by a compact half-wavelength dipole antenna which is held in place between the magnetic shields and one of the vacuum chamber windows closest to the trap.

IV. Spectroscopy

After loading and cooling ions, to form a Coulomb crystal, we probe the clock transition using the experimental sequence shown in Fig. 4. When the microwaves are switched off, ions are optically pumped into the $F = 0$ ground ("state prep" in the figure). Then a microwave π-pulse excites the ions to the $F = 1$, $m_F = 0$ level. The $m_F = \pm 1$ states are shifted off resonance by a bias field of ~7 μT. After the microwaves are switched off again, we switch the laser back on and detect a fluorescence signal with the PMT that is proportional to the number of ions that made the transition. We step the microwave frequency between iterations of this sequence to scan over the clock transition

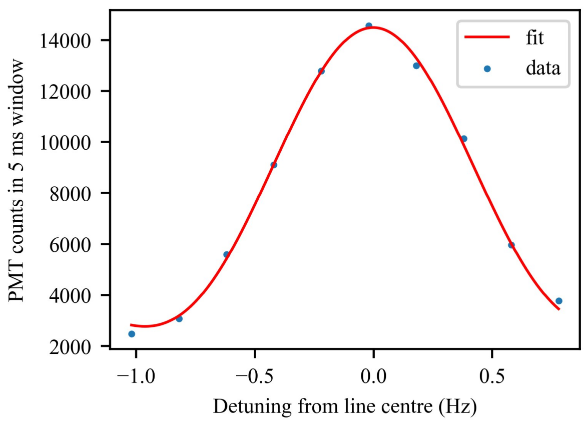

Fig. 5. Rabi spectrum taken with microwave pulse duration of 900 ms. The scan range is narrow, so it omits the side lobes of the Rabi lineshape.

and plot the PMT counts against frequency to see the probe-time limited spectrum shown in Fig. 5.

To lock the clock, we repeat this sequence in an A-B-B-A fashion, which removes, to first order, linear drifts in the OCXO and atomic signal level, where "A" indicates we are probing with the microwave frequency set to one side of the fringe and "B" indicates the other side. The centre of the fringe is calculated in software and the clock output is adjusted accordingly. To assess the frequency stability of the clock, its output is compared to a UTC(NPL)-steered hydrogen maser signal. We then calculate the overlapping Allan deviation, which is plotted for a clock run in Fig. 6. The OADEV averages as approximately $3.2 \times 10^{-12}/\sqrt{\tau}$ between 30 and 10,000 seconds.

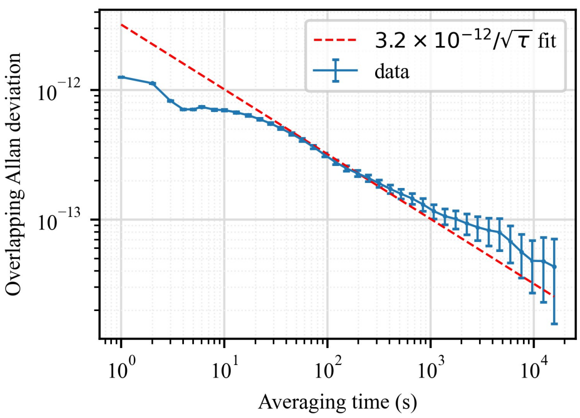

Fig. 6. Clock stability measured vs. NPL hydrogen maser. The fit is to the data points between 45 and 16,000 seconds.

V. Conclusions and Next Steps

To conclude, we have built a lab demonstrator of an ytterbium ion microwave clock, which includes a new physics package design, which we describe in this paper. Initial spectroscopy and clock stability measurements have been presented.

We intend to further optimise the clock stability by increasing the signal to noise ratio of the detected ion signal and characterising sources of phase noise. The next steps towards our goal of a transportable clock are to build and test new compact subsystems, including the laser systems and optics, control electronics and power supplies.

Acknowledgment

The authors would like to thank Ulas Gokay and Setnam Shemar for reviewing the manuscript.

References

[1] S. Mulholland *et al.*, "Laser-cooled ytterbium-ion microwave frequency standard," *Appl. Phys. B Lasers Opt.*, vol. 125, pp. 198, 2019.

[2] S. Mulholland *et al.*, "Compact laser system for a laser-cooled ytterbium ion microwave frequency standard," *Rev. Sci. Instrum.*, vol. 90, pp. 033105, 2019.

[3] N. C. Xin *et al.*, "Laser-cooled $^{171}Yb^{+}$ microwave frequency standard with a short-term frequency instability of $8.5\times10^{-13}/\sqrt{\tau}$" *Opt. Express*, vol. 30, pp. 14574, 2022.

[4] S. Mulholland, "Development of a portable laser-cooled ytterbium ion microwave atomic clock", PhD Thesis, University of Oxford, 2019.